This is a peer-reviewed, accepted author manuscript of the following conference paper: Miljanović, M, Kearns, M & Stewart, BG 2024, Simulation of PD RF EM wave propagation in different MV bus bar compartment configurations. in 23rd International Symposium on High Voltage Engineering (ISH 2023). IEEE, Piscataway, NJ, pp. 692-698. https://doi.org/10.1049/icp.2024.0603

SIMULATION OF PD RF EM WAVE PROPAGATION IN DIFFERENT MV BUS BAR COMPARTMENT CONFIGURATIONS

Mijodrag Miljanović[1], Martin Kearns[2], Brian G Stewart[1*]

[1]The Institute of Energy and Environment, Depart. of Electronic & Electrical Engineering, University of Strathclyde, Glasgow, UK
[2]EDF (UK), 191 Hope St, Glasgow, UK
**brian.stewart.100@starth.ac.uk*

Keywords: SIMULATION, SWITCHGEAR, PARTIAL DISCHARGE, ELECTROMAGNETIC WAVE PROPAGATION, FINIT ELEMENT METHOD

Abstract

Monitoring of partial discharge (PD) in air-insulated medium voltage (MV) switchgear can reveal potential insulation failure. There is still clarification needed to understand the most effective placement of RF probes, especially along extended MV switchgear line-ups. In this work a simulation study was performed to investigate the differences between the PD propagation characteristics of electromagnetic (EM) waves in one single busbar and a triple line-up of bus bar compartments.. A finite element method (FEM) bus bar compartment model is created and simulations are performed in Comsol Multiphysics. By applying PD sources at specific locations on particular phases, RF signals are recorded along the compartment surfaces. Based on created signal energy interpolation maps, the potential best sensor position placement areas of RF sensors is revealed for each PD case for the different compartment structures. The study reveals that for the sake of PD signal propagation studies PD within a single compartment model may produce similar PD sensor positions to PD within a central busbar chamber within a triple compartment.

1 Introduction

1.1 Partial Discharge Detection

Partial discharge (PD) monitoring in medium voltage (MV) and high voltage (HV) equipment can reveal potential insulation degradation [1]. Generally, a specific level of PD may exit even if there is no insulation failure due to environmental conditions such as increased humidity or dust.

Two main methods for PD detection exist. These are differentiated between conventional and non-conventional approaches. The conventional approach is mainly applied for system tests at the end of the manufacturing process or for commissioning purposes on site. The particular test is described by the IEC EN 60270:2001 Standard. The non-conventional approach is described in IEC technical specification PD IEC/TS 62478:2016. These methods recommend the need for a continuous monitoring technique implementation within systems. The technical standard covers different monitoring techniques, among which the RF detection method is described [2].

1.2 Partial Discharge Monitoring in MV Switchgear

Since there is a future need for improved condition-based monitoring of power systems, the application of RF methods has come more into research focus [3]. In terms of MV switchgear, PD experiments were conducted as in [4] by applying sensors at different locations of switchgear line-ups, where the influence of different switchgear compartments on the electromagnetic (EM) wave propagation was studied. Nevertheless, the work also suggests further investigation and understanding of EM wave propagation of RF signals within switchgear chambers.

In [5] a simulation study was conducted for a single switchgear where EM wave propagation was investigated. UHF probes were applied at different positions to investigate the influence of different PD locations. Throughout the work it was shown that captured probe signals differ when different PD locations are applied

Based in previous published research, there is still need for the estimation of the optimum positions for PD sensor location for different internal switchgear structures. Further, literature investigations are usually split into two different paths, experimental and simulation studies. The objective of the current work is to support the investigations of RF signal propagation based on simulation studies.

1.2 Research Outlook

In addition to the above, the bus bar compartment of a medium voltage switchgear seems to be sensitive to PD failures [6]. Usually, internal parts are not easily accessible and their monitoring difficult. As a contribution to this research area, EM wave signal propagation characteristics will be studied in in a single compartment and a three compartment switchgear line-up. A comparison will be conducted in order to determine also if simulation modelling requires the entire line-up system

for EM wave propagation studies or if it would be sufficient to perform studies on a simplified single compartment.

In the following section, the methodology of the conducted work will be presented. PD simulation results will then be shown and in the last section conclusions will be drawn.

2. Methodology

A three-dimensional (3-D) finite element method (FEM) is adopted to create a single and a triple (line-up) MV bus bar compartment model. PD sources are implemented in the form of a current pulse based on the Gaussian pulse function on three different phase positions in the bus bar compartments. In the simulations, RFI probes are placed along the compartment inner wall surfaces and EM fields are recorded in the time domain. Based on this data, interpolation maps of the potential high signal energy regions along the surfaces are created and compared. From the interpolation maps the best or optimum signal energy sensor placement position are estimated along the bus bar compartment.

2.1 Switchgear Compartment Model

The bus bar compartment modelling is based on an arbitrary switchgear, as shown in Fig. 1. It comprises side walls, made of steel, bus bar conductors made of copper and bus bar supports made of epoxy resin.

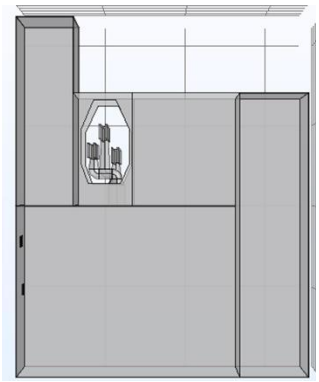

Fig. 1 Arbitrary switchgear model and bus bar compartment

2.2 PD Source

The PD source is implemented based on the Gaussian pulse function, as described by Eq. (1), according to [7]. An example plot of a current pulse is given in Fig. 2.

The peak current is represented by I_0 set to 1A amplitude. The parameter t1 determines the time in the simulation the PD current pulse occurs. The term τ represents the pulse width parameter, which is set to 0.42 ns in order to achieve a 1ns PD pulse width as shown in Fig. 2.

$$i_{PD}(t) = I_0 * e^{-[\frac{(t-t1)^2}{2*\tau^2}]} \qquad (1)$$

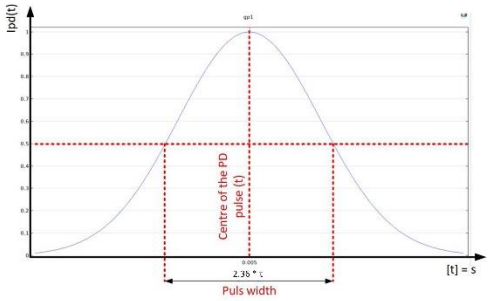

Fig. 2 Example PD pulse function for a 1ns pulse width

Using the parameters above, different PD pulse shapes can be established and thus different PD types initiated. For the particular simulations below, the PD pulse according to Eq. (1) and shown Fig. 2 is applied.

2.3 Sensor and PD Positions

For simulation of PD detection, 27 probe positions are distributed along the surface wall of the bus bar compartment as indicated by black arrows in Fig. 3. The density of sensor positions is chosen so as to be able to create effective signal energy interpolation maps.

For each simulation a PD source is separately applied in each bus bar compartment. The positions of the PD sources within the model are represented by so-called lumped ports with a dimension of 10x10mm at each bus bar support. The lumped port represents particular electrodes along which the PD current density pulse is driven based on the Gaussian function.

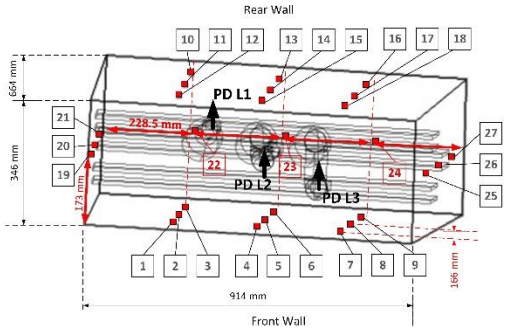

Fig. 3 Bus bar compartment model with indicated probe positions along compartment surface and PD positions at bus bar supports

2.3 Simulation Set-Up

Simulations are carried out in the time-domain using the so-called transient electromagnetic wave (temw) feature in Comsol Multiphysics. The Pardiso solver with Generalized-alpha time stepping is applied to solve the equations – this is a common solver for such studies [8]. The simulation time step is set to 1 ps whereas the output time for the results is set to be every 0.1 ns. The duration of the simulation is set to 400 ns so as sufficient signal energy can be evaluated over time..

2.3 Generation of Interpolation Maps

The data gathered from the simulation process is stored into csv-files. The data is then read into Matlab and the scattered interpolant technique is applied using the linear interpolation method to create the signal energy maps. The signal energy is calculated according to Eq. (2).

$$E_{signal} = \sum_1^n |x[\Delta T_n]|^2 \qquad (2)$$

In the first step, the signal energy is calculated based on the stored data. In the second step, the interpolation maps are generated using the signal energy information and the interpolation algorithm.

3 Simulation Results

3.1 Single Compartment

In the following figures the results are shown for PD on three different bus bar supports. The region with the highest signal energy can be recognised by the overlayed interpolation map on the bus bar compartment. In addition, the position where the highest signal energy occurs is identified by a small red star.

In Fig. 4, the signal energy interpolation map is shown for the case of PD on phase L1. It can be seen that the highest signal energy occurs at the probe position P14. The position is on the rear wall of the compartment, which may be expected due to the close vicinity to the PD source.

In Fig. 5, the signal energy interpolation map is shown for PD on L2. At first sight, compared to the previous case, it can be noticed that the highest signal energy spot is nearly at the same position in the middle of the compartment. The highest spot occurs again at probe position P14. It can be also seen that in this particular case the signal energy profile has a concentric shape at the rear wall around the probe position. In addition, there is also a higher sensitivity area at the top wall of the compartment. Due to the proximity of the bus bar support L2 to probe P14 within the compartment, the highest signal energy intensity thus appears near the same location as in the case of L1.

In Fig. 6, the signal energy interpolation map is shown for PD on phase L3. The highest signal energy appears at probe position P8.

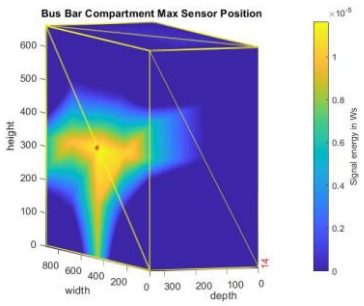

Fig. 4 Rear wall view of bus bar compartment, interpolation map for PD on L1, of single compartment (P14)

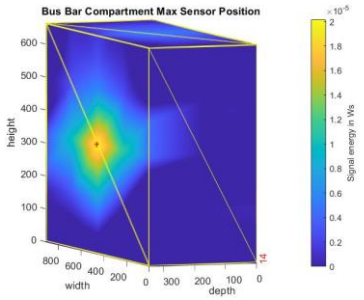

Fig. 5 Rear wall view, interpolation map for PD on L2, of single closed single compartment (P14)

Due to the position of the bus bar support to the right-hand side of the compartment, again, the highest energy area appears in the proximity of the PD source. Interestingly, in this particular case there is also a higher signal sensitivity band occurring in the middle of the compartment wall, which seems to be at the same height as the bus bar conductors within the compartment.

In Fig. 7, the maximum probe signals are shown for the three previous presented scenarios on the same plot. The signals represent the captured electric fields for the different PD activities on the particular phases. As it can be seen the signals are in the same amplitude range. The signal signal frequencies lie around 0.3 GHz which corresponds to the UHF range.

In Fig. 8 the captured signals are represented over a ttime period of 10 ns. With reference to 5 ns, when the PD pulse occurs on each phase, all of the three first signal peaks are slightly shifted in the time axis.

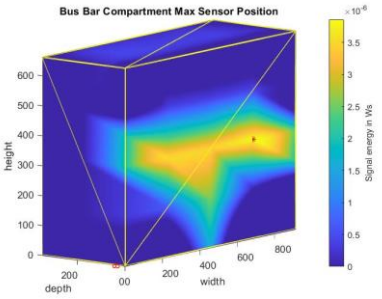

Fig. 6 Front wall view, interpolation map in case of PD on L3, of closed single compartment (P8)

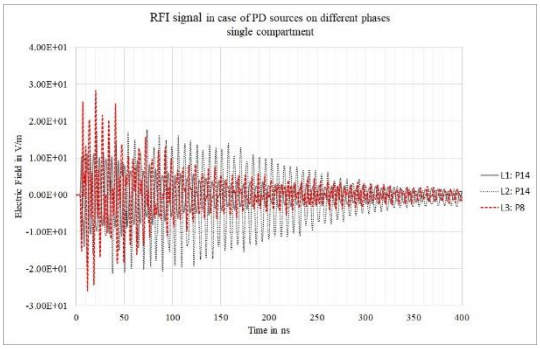

Fig. 7 Graphs of the probe positions where highest signal energy is detected in case of PD on L1, L2 and L3 separately.

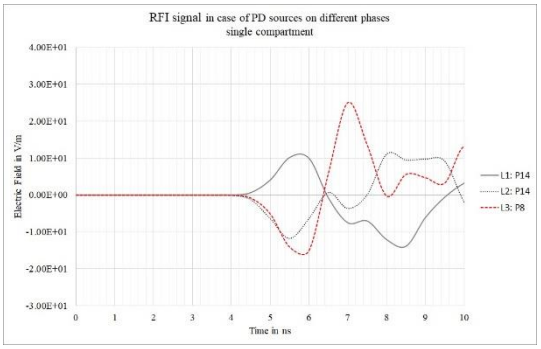

Fig. 8 Extracted graphs for a detail view of the probe positions where highest signal energy is detected in case of PD on L1, L2 and L3 separately.

Taking the signal shift for example of the PD signal L1 into account, which is of around 0.7 ns and the wave propagation time of 0.3 m/ns, the distance can be calculated from the PD source to the compartment wall where the RF probe is placed. For the above parameter stated, the distance between PD on L1 and the probe that captured the signal is around 0.21 m which corresponds to the structure dimensions. The same can be calculated for the other two PD sources, PD on L2 and PD on L3, which verifies the particular model.

3.1 Triple Line Up Compartment

In Fig. 9 the interpolation map is shown for PD on L1 for the middle compartment in the triple line up arrangement. It can be seen, the highest energy area appears to occur at the same probe position, P14, as determined from the single compartment model in Fig. 4. In addition, a higher signal energy region band appears in the middle of the compartment. Comparing Fig. 4 of a single compartment structure and Fig. 9, it seems that there is minimal influence of the structure position where the highest signal energy appears. The difference is in the signal intensity, where the signal energy seems to be around an order of magnitude smaller compared to the single compartment.

In Fig. 10 the signal electric fields of the PD in the single compartment and the PD in a triple line up are displayed for the same bus bar support L1. In both cases it can be seen that the first signal peaks appear at the same time, which means that the distance from the particular probe to the PD source is the same for both signals. In contrast, the signal from the triple compartment seems to be lower. It appears that the study could be conducted on a single compartment and the main sensor position results transferred to the line-up structure. This potentially would save modelling time for the scenarios depicted. This of coursem ay not be true for PD locations not on the positions considered in this study.

In Fig. 11 the interpolation map is presented for the triple line-up chamber for PD on phase L2 in the middle compartment. It can be seen that the highest signal energy spot occurs at probe position P14, which is close to the PD source. The signal energy intensity is of an order of magnitude lower compared to the single compartment case in Fig. 5. In addition, it can be also seen in Fig. 11 that there is a smaller concentric signal energy area around the particular probe, compared to the single compartment case. In addition a thin high signal energy band can be also recognised in the middle of the compartment going through the centre of the circular profile. It seems that the position of the particular high energy band is at the same height as the bus bar conductors within the compartment. This might be due to the concentration of EM wave propagation along the copper conductors. On the other hand, there is also a slightly higher signal energy spreading around the entire rear wall structure and going vertically from the top compartment to the middle compartment. A similar shape appears also in case of the single compartment when PD L2 is active, seen in Fig. 5.

The particular electric field graphs in case of PD on phase L2 in the single and triple line-up are shown in Fig. 12. It can be seen that the first signal peaks are around the same amplitudes whereas the overall signal in the single bus bar compartment remains with a higher amplitude over the simulation time. Generally, it can be seen that in case of the triple compartment the signal decay is higher whereas in the case of the single compartment the signal is relatively constant up to 150 ns, decaying gradually after that period. This could be due to the smaller space provided in the single compartment and the same energy applied for both PD. Nevertheless, it seems that for a PD source on L2, either in a single compartment or triple line-up, there is minimal influence of the outcome of the signal energy map and hence the potential best placement of the sensors. Therefore, as before for L1 instead of modelling an entire line-up structure, the studies could potentially have been conducted on a single compartment model.

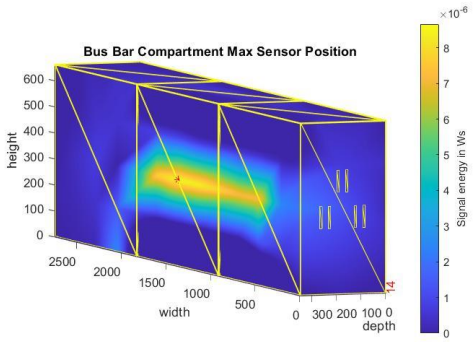

Fig. 9 Interpolation map in case of PD on L1, of open middle compartment in a triple arrangement (P14)

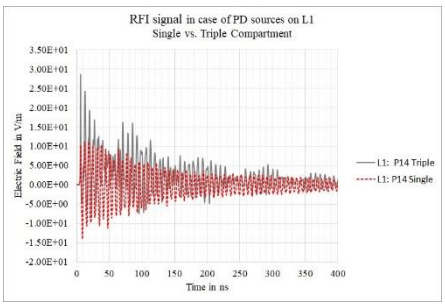

Fig. 10 Signal graphs of probe positions of highest signal energy detected for PD on phase L1 in single and triple compartment

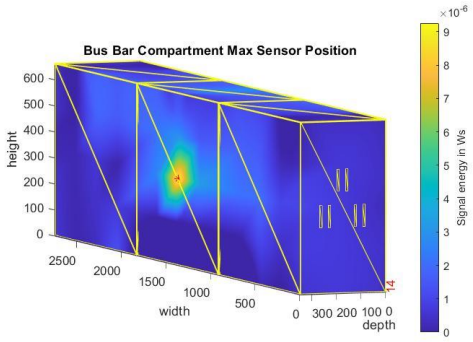

Fig. 11 Interpolation map in case of PD on L2, of open middle compartment in a triple arrangement (P14)

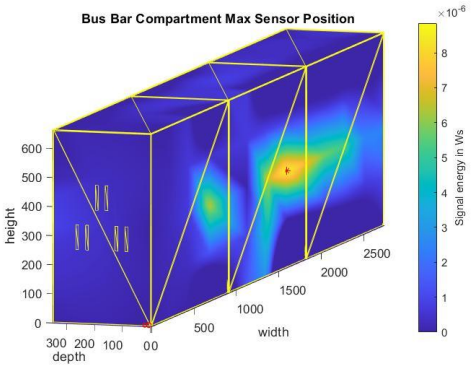

Fig. 13 Interpolation map in case of PD on L3, of open middle compartment in a triple arrangement (P8)

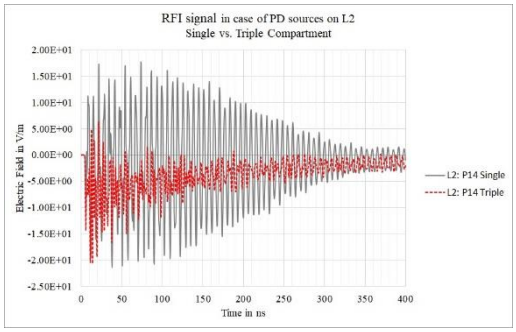

Fig. 12 Signal graphs of probe positions of highest signal energy detected for PD on phase L2 in single and triple compartment

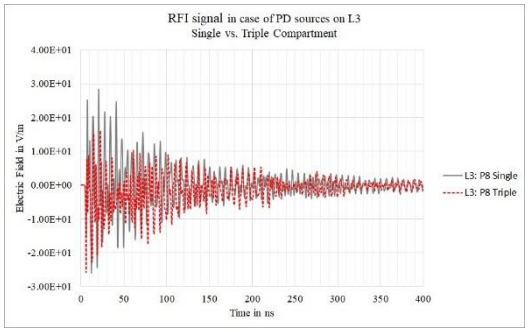

Fig. 14 Signal graphs of probe positions of highest signal energy detected for PD on phase L3 in single and triple compartment

In Fig. 13. the triple line-up bus bar compartment is shown for PD on phase L3. It can be seen the highest energy intensity appears at probe position P8. Interestingly, comparing this with the case of the single compartment, in Fig. 6, the highest energy sensitivity occurs at nearly the same position. In addition to that, it seems that the higher signal energy region follows the bus bar conductor since there is a particular higher energy band reflected at the middle part of the interpolation surface, as in the cases of PD on phase L1 and L2. Therefore, similar to previous cases the outcome result does not change comparing the simulation with the single compartment model. What changes is the signal energy captured and the shape of the interpolation map, but the probe position with the highest energy detected remains the same.

In Fig. 14 the electric fields plots are displayed when PD occurs in the single and the middle compartment in the triple line-up structure. Generally, it can be seen that the signal in the single compartment possesses a higher amplitude comparted to the one of the triple line-up compartments. This is due to the same energy of the PD source in both cases applied and the fact that in case of a triple compartment there is a wider space for the signal to dissipate with less close refections. Again, it can be noticed that the signal peaks at the beginning of the capturing are overlayed which suggests the probes are at the same distance from the PD source. The RF plot for PD on L3 in the single compartment tends to have higher amplitudes at the beginning of the signal recording. This is quite reasonable since the signal energy captured on the particular probe position for the PD source in the single compartment is higher, as can be seen when comparing Fig. 13 with Fig. 3.

Another interesting point for note is that when simulations are run over smaller simulation time windows, for example 100 ns, the interpolation maps are very similar. Thus, even when reducing the simulation times, the probe positions of the detected high energy regions remain similar for all PD cases and compartments. As an example, the signal energy interpolation map is shown in Fig. 15 for the case of the PD source on L1 and simulation time of 100 ns. Comparing with Fig. 9, where the simulation time is 400ns there is little difference. The highest signal energy is at the same position of P14. What changes is the signal energy, which is around 75% less for case of the 100ns window.. The same was found for the cases where PD occurs on L2 and L3.

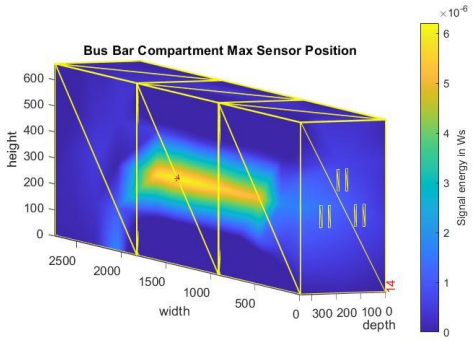

Fig. 15 Interpolation map in case of PD on L1, of open middle compartment in a triple arrangement for simulation time of 100 ns, as an example (P14)

4 Conclusions

From the simulation studies for the case of PD in a particular compartment, the highest signal energy remains along the surfaces of the specific compartment. It seems there is little difference when focusing on a single compartment or on the middle compartment in a triple line-up structure. For both compartment model the signal propagation characteristics provide similar optimum sensor location positions.

Based on the investigations undertaken of potential higher signal sensitivity areas for RF signals it appears foir the cases in question, sufficient to run the simulations based on a single compartment. This enables to efficient simulation potentially saving simulation time and calculation memory. In addition it was also shown that the results remains similar by reducing the simulation time window to a lower value.

The results also indicate little change in the outcome of the interpolation maps of optimum probe position. For example, results for PD sources on phase L1 and phase L2 indicate, the highest signal energy is detected at the same place on the rear wall surface of the compartment at probe position P14 regardless if it is single or a triple line up structure. Similarly for the PD source on L3, the highest signal sensitivity appears on the opposite site, at the front wall of the compartment at the position P8.

Rom the investigated potential PD sensor interpolation maps it can be seen the higher sensitivity regions are mainly concentrated on the surface walls at the same height as the bus bar conductors within the compartment. Knowing that and the fact that most failures caused by PD are concentrated around the bus bar supports and conductors due to the so-called triple junction point, the application and positioning of such sensors at these locations for monitoring purposes in the field maty produce the optimised signal detection energies..

5 Acknowledgements

This work was funded by EDF Energy UK.

6 References

[1] M. D. Judd, Li Yang and I. B. B. Hunter, "Partial Discharge Monitoring of Power Transformers Using UHF Sensors. Part I: Sensors and Signal Interpretation," IEEE Electrical Insulation Magazine, vol. 21, no. 2, pp. 5-14, March-April 2005, doi: 10.1109/MEI.2005.1412214.

[2] Joint Work Group A3.32/CIRED, "Non-Intrusive Methods for Condition Assessment of Distribution and Transmission Switchgear", CIGRE/CIRED, August 2018.

[3] W. Lian, T. Zhao, "Design of Insulation Online Monitoring and Anti-Condensation Control System for Distribution Switchgear", Academic Journal of Engineering and Technology Science, ISSN 2616-5767 Vol.4, Issue 2: 45-51, 2021, DOI: 10.25236/AJETS.2021.040207

[4] C. Pestell, D. Caves and J. Bowen, "Qualitative analysis of partial discharge radio frequency emission propagation in medium voltage metal-clad switchgear," 2017 Petroleum and Chemical Industry Technical Conference (PCIC), Calgary, AB, Canada, 2017, pp. 185-194, doi: 10.1109/PCICON.2017.8188737.

[5] J. Li, J. Wang, Y. Shi, H. Wang and T. Zhao, "Simulation of Propagation Characteristics of PD UHF Signals inside and outside of Switchgear," 2020 IEEE 3rd Student Conference on Electrical Machines and Systems (SCEMS), Jinan, China, 2020, pp. 365-368, doi: 10.1109/SCEMS48876.2020.9352280.

[6] J. E. Smith, G. Paoletti and I. Blokhintsev, "Experience with on-line partial discharge analysis as a tool for predictive maintenance for medium voltage (MV) switchgear systems," Record of Conference Papers. Industry Applications Society. Forty-Ninth Annual Conference. 2002 Petroleum and Chemical Industry Technical Conference, New Orleans, LA, USA, 2002, pp. 155-161, doi: 10.1109/PCICON.2002.1044997.

[7] T. Zhao, M.D. Judd, B.G. Stewart, "Time Dependent Simulation of PD Electromagnetic Wave Propagation", Annual Conference on Electrical Insulation and Dielectric Phenomena (2020): CEIDP 2020.

[8] Comsol Multiphysics Reference Manual, Version: COMSOL 5.5, 2019